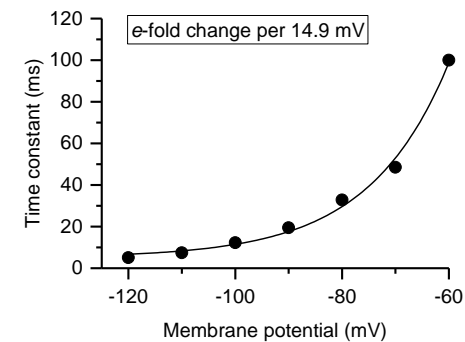
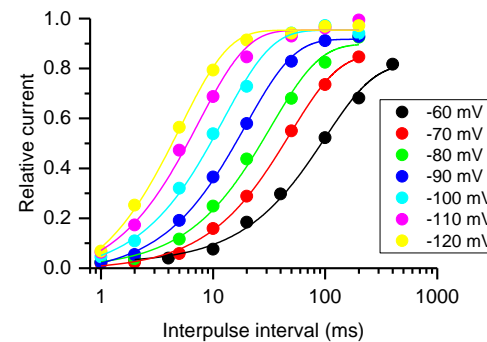
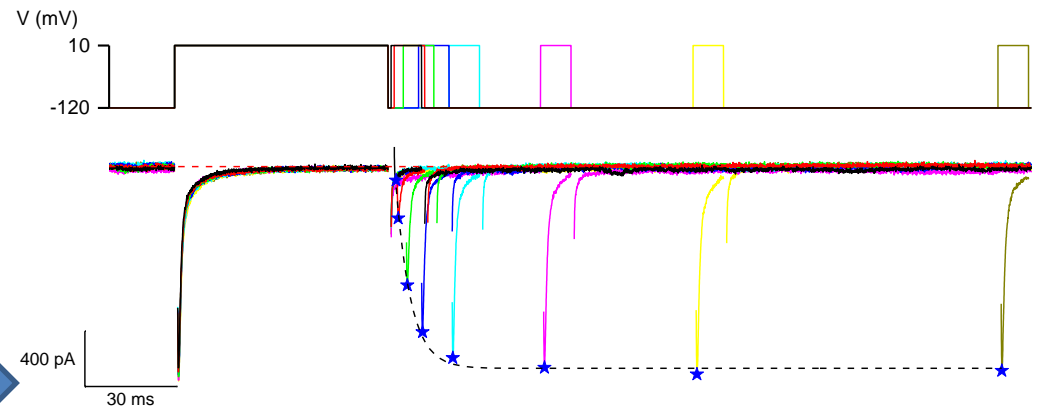
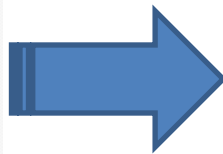
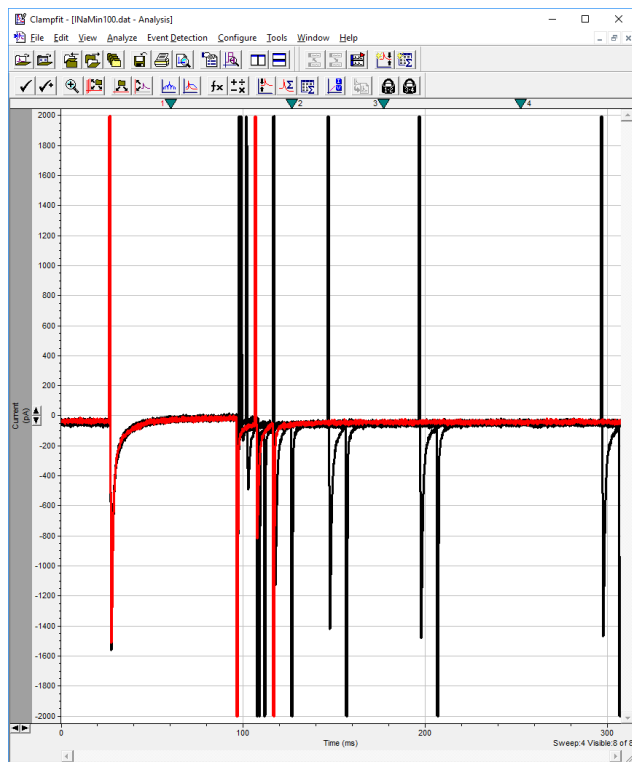


# Advanced pClamp Analyzer

## Quick Start



*by Alex Zholos*

# Case studies illustrating several scenarios, in which the **Advanced pClamp Analyzer** can be used



## Benefits of the tools:

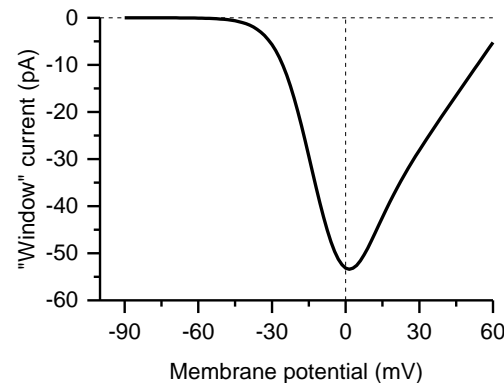
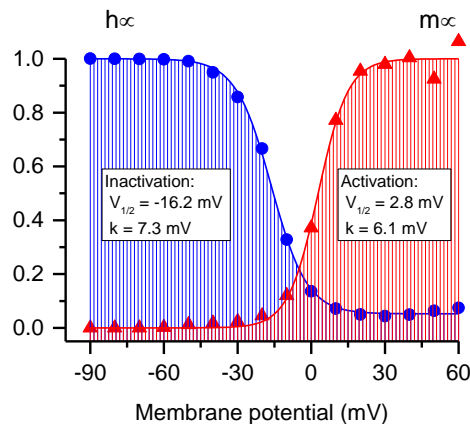
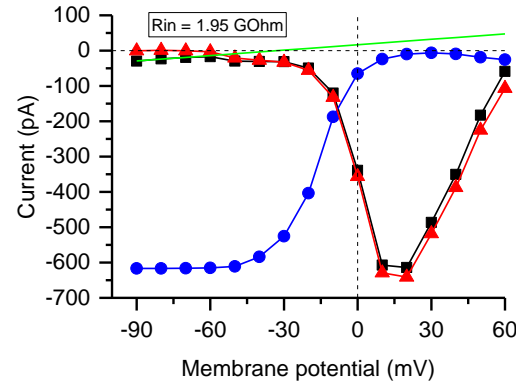
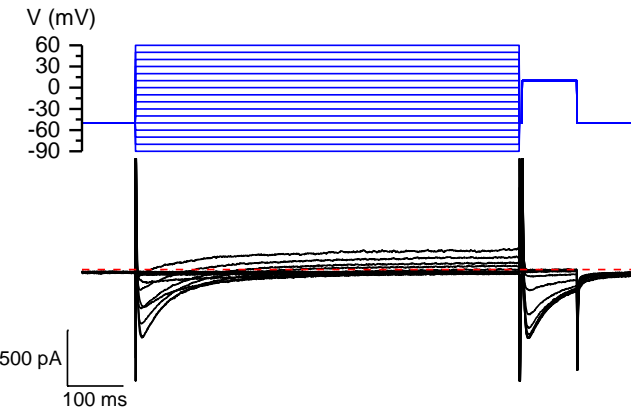
- ❖ Suitable for any type of voltage-dependent or receptor-operated ion channel currents
- ❖ Can handle data acquired using both voltage steps and voltage ramps
- ❖ Ensure fast, reliable, human error-free data analysis
- ❖ Include user interface to enhance their versatility
- ❖ Produce publication quality graphs


## Sample files provided:

1. WinCurrent.abf
2. TRPM8\_heating\_1C.abf
3. IKa\_Recovery.dat
4. INaMin60.dat ... INaMin120.dat
5. INa\_TTX.dat
6. INa\_Wash.dat
7. CCh\_DR.abf

**Sample files** are saved in Apps folder: **\\Advanced pCLAMP Analyzer\\Samples**

# 1. “Window” voltage-dependent calcium current



Click  and select file:

**WinCurrent.abf**

Click 

Dialog box: Activation Epoch

Enter 2

Dialog box: Inactivation Epoch

Enter 4

Dialog box: Enter Erev

Automatically estimated value is displayed (63.59887).

Try 67 instead

*NB* the calculations can be repeated for different Erev without the need for file re-import

**Layer 1** shows voltage protocol.

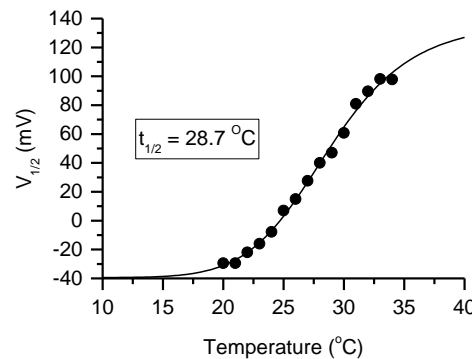
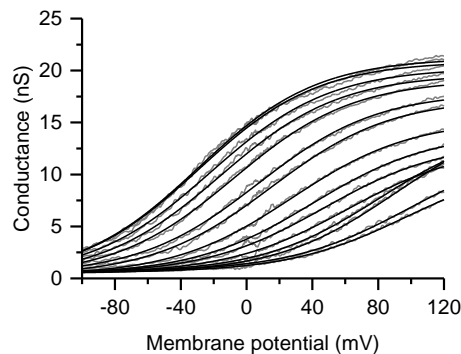
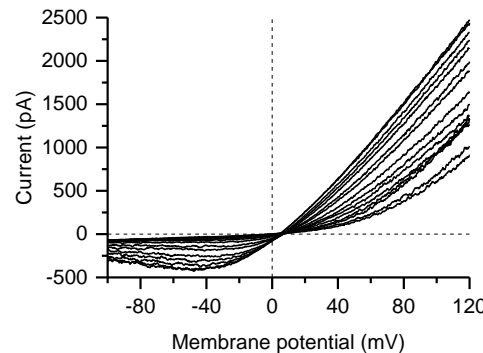
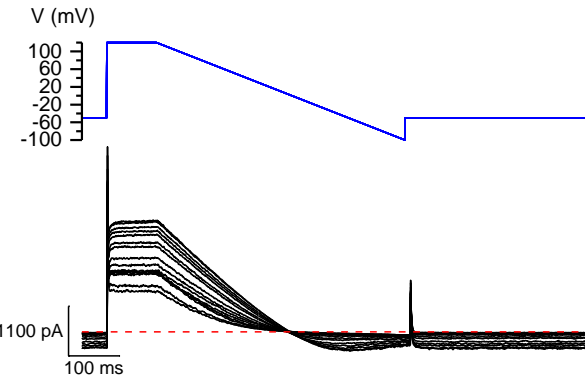
**Layer 2** shows superimposed voltage-dependent calcium current traces acquired using the above shown voltage-step protocol.

**Layer 3** shows current-voltage (I-V) curve (black squares, data from Epoch 2), steady-state inactivation curve (blue circles, data from Epoch 4), estimated leak current (green line), leak-corrected I-V curve (red triangles), and calculated input resistance value (Rin in GOhm).

**Layer 4** shows steady-state activation (red triangles) and inactivation (blue circles) data points fitted by Boltzmann relations (continues lines), with corresponding best-fit parameters characterizing voltage dependence of calcium channel activation and inactivation indicated.

**Layer 5** displays the calculated voltage-dependent calcium “window” current, predicted by the overlap of the steady-state channel activation and inactivation. All parameters are saved in the “Results” workbook.

## 2. Investigation of temperature-dependent shift of the voltage activation range of the menthol and cold receptor TRPM8



Click  and select file:

**TRPM8\_heating\_1C.abf**

Click 

Dialog box: Perform Boltzmann fit?

Click Yes

Skip every N points – “0”

Dialog box: Fit with shared slope? “

Click Yes

Dialog box: Define temperature range

Click Ok to confirm the default values:

Initial temperature 20

Temperature increment 1

**Layer 1** shows voltage protocol.

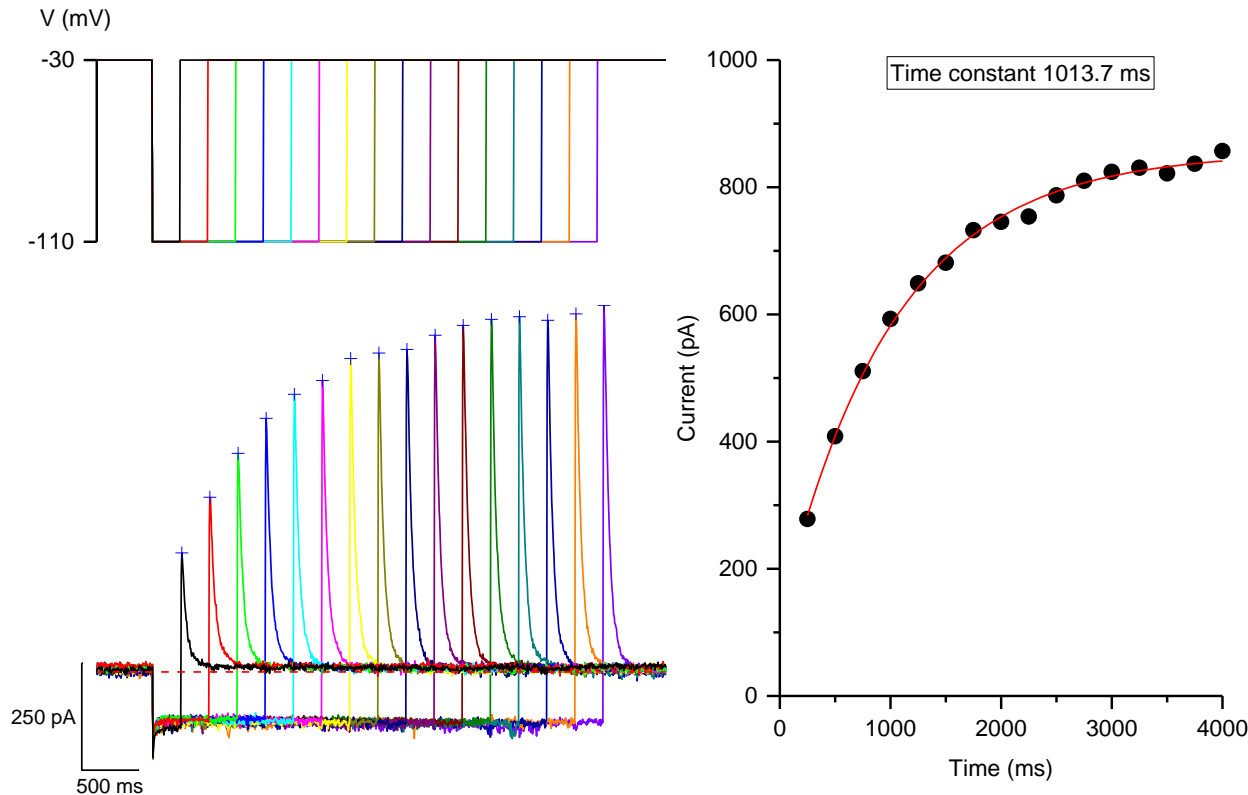
**Layer 2** shows superimposed TRPM8 current traces.

**Layer 3** shows I-V curves measured at different temperatures, ranging from 20 °C to 34 °C with 1 °C increment.

**Layer 4** shows corresponding conductance curves calculated as  $G=I/(E-E_{rev})$ . Reversal potential values for each trace measured by linear regression of data points within  $\pm 1$  mV of current reversal are saved in the “Erev” workbook.

**Layer 5** plots the best-fit values of the potential of TRPM8 half-maximal activation ( $V_{1/2}$ ) depending on temperature. The values are fitted by sigmoid function with temperature producing half-maximal shift of  $V_{1/2}$  indicated in the label.

### 3. Recovery from inactivation – neuronal $I_A$ potassium current



Click  and select file:

**IKa\_Recovery.dat**

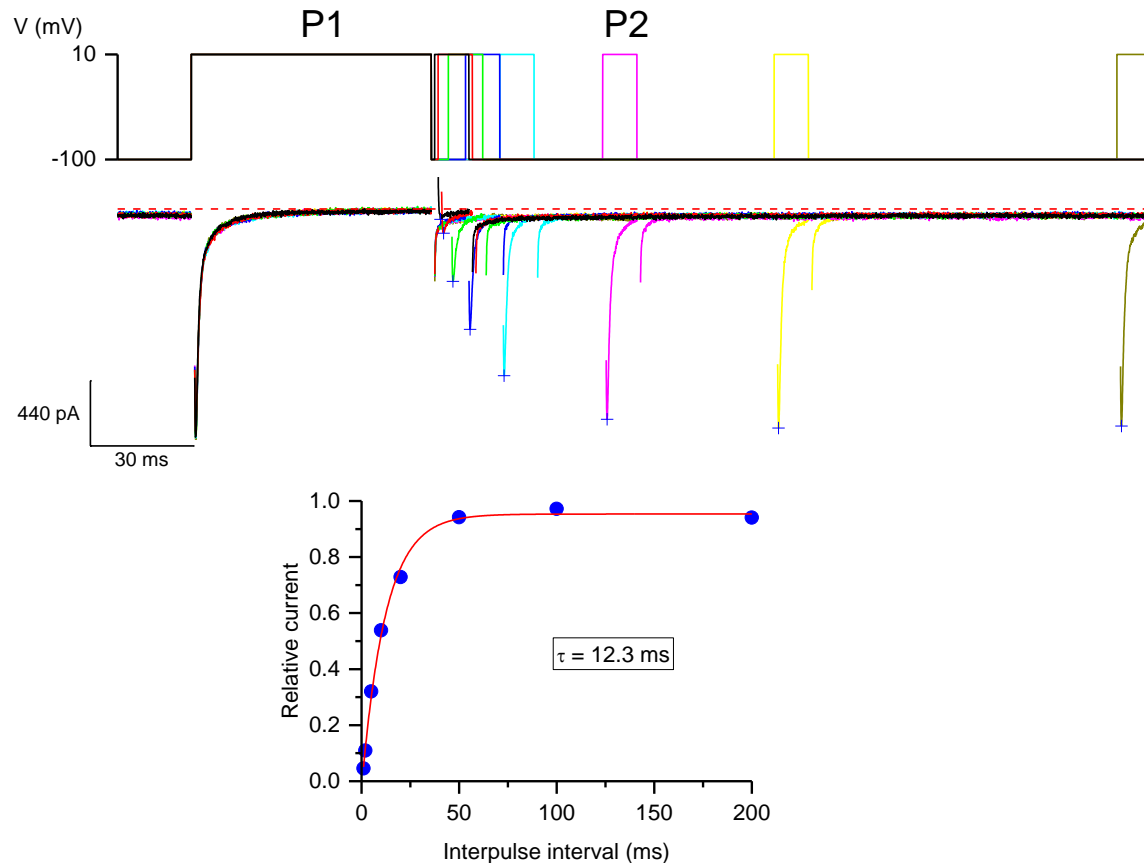
Click 

**Layer 1** shows voltage protocol. Note that fast A-type potassium channels are fully inactivated at the holding potential of -30 mV, while they are not inactivated at the test potential of -110 mV. Voltage steps to -110 mV of increasing duration thus progressively remove channel inactivation, as evaluated by stepping back to -30 mV.

**Layer 2** shows corresponding superimposed potassium  $I_A$  current traces.

**Layer 3** plots current amplitude as function of the duration of the voltage step to -110 mV. Data points were fitted by single exponential function with the time constant for the process of  $I_A$  recovery from inactivation shown in the label.

# 4. Recovery from inactivation – voltage-dependent sodium current



Click  and select file:

**INaMin100.dat**

Click 

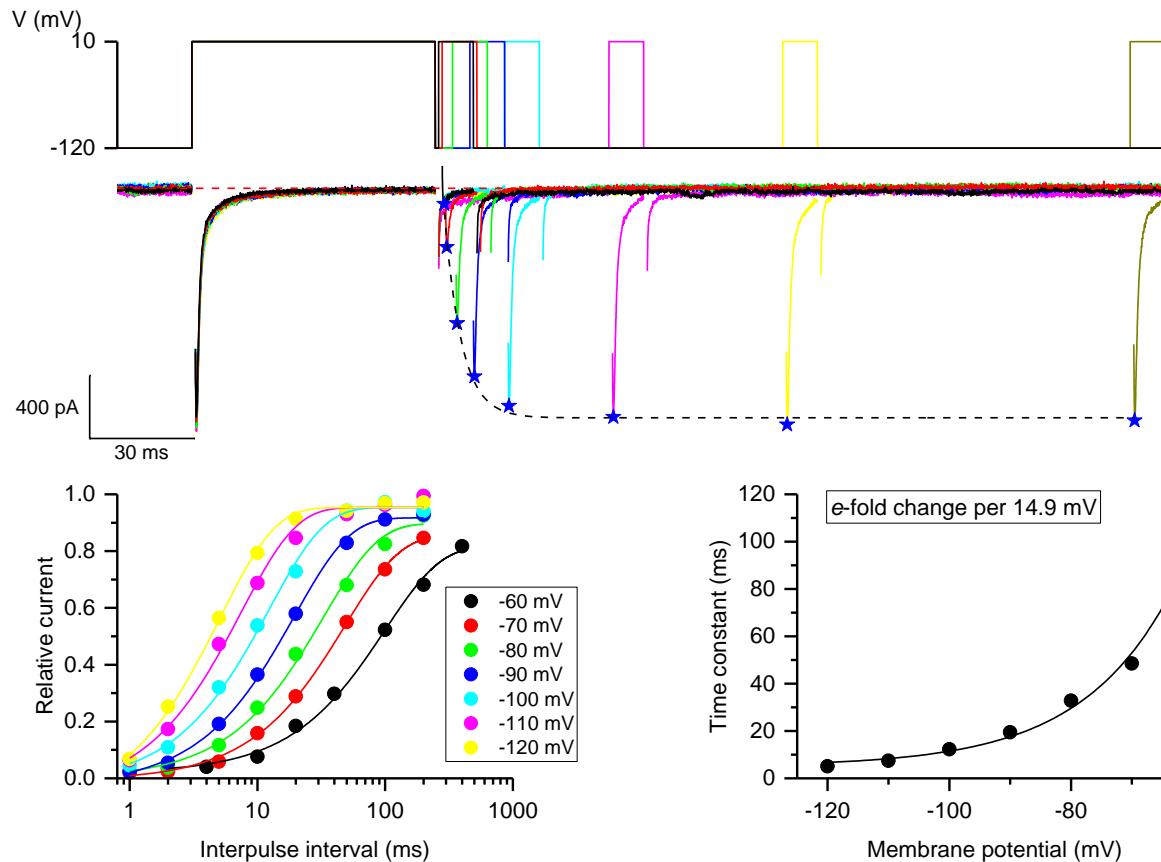
Dialog box: Exclude capacitive current  
Enter 1

**Layer 1** shows voltage protocol. Here the “classical” double pulse protocol was used, in which the first voltage step (conditional step - P1) causes channel inactivation, while the second pulse (test step - P2) is applied to evaluate the extent of  $I_{Na}$  recovery from inactivation during the inter-pulse interval. The latter is incremented to follow the time of recovery from inactivation.

**Layer 2** shows superimposed  $I_{Na}$  current traces.

**Layer 3** plots normalised current amplitude (i.e. ratio of current amplitudes P2:P1) as function of the inter-pulse duration. Data points fitted were by single exponential function to define the time constant for the process of  $I_{Na}$  recovery from inactivation (shown in the label).

# 5. Investigation of the voltage dependence of the rate of recovery from inactivation – $I_{Na}$



Click  
files:



and select multiple

**INaMin60.dat ... INaMin120.dat**

Click

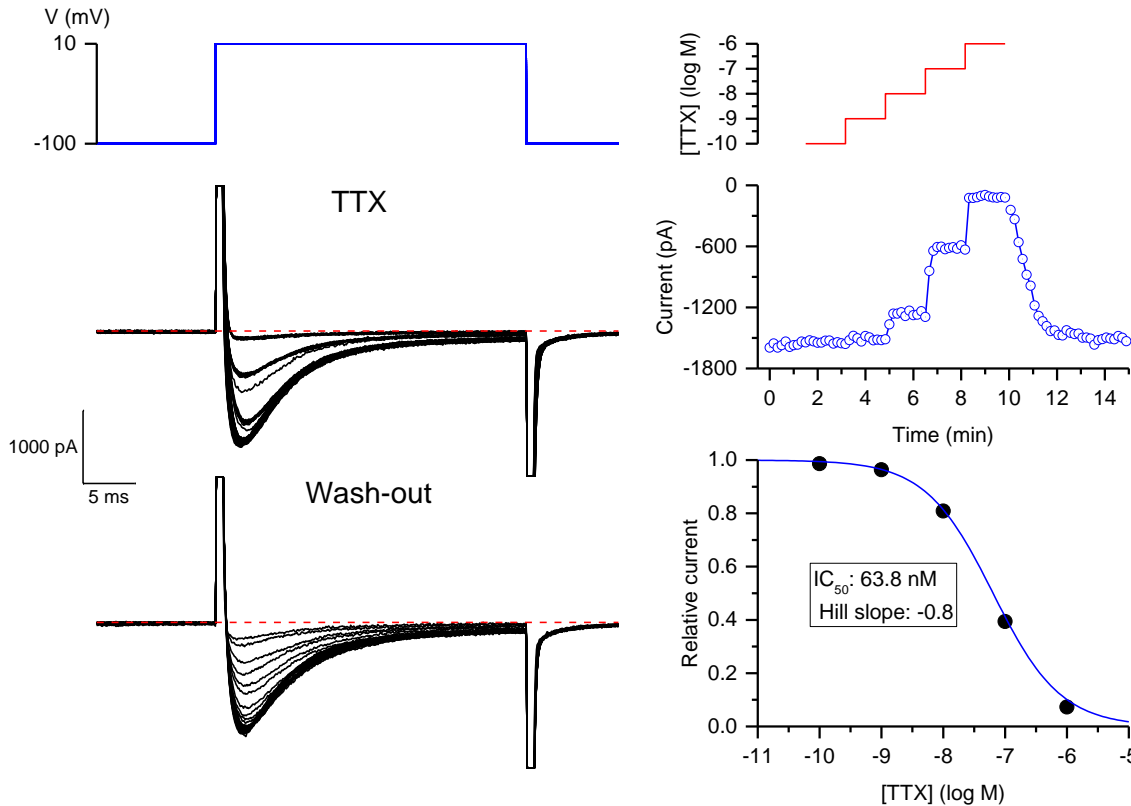


Dialog box: Exclude capacitive  
current  
Enter 1

**Layer 1 & Layer 2** show examples of voltage protocol and current traces recorded in the same cell at one of the inter-pulse potentials used (here steps from -120 to -60 mV with a 10 mV increment, exemplified at -120 mV), similarly to the above described case 4. After completing the data analysis at each test potential, the script pauses for 5 s to allow visualization of the individual results, which are saved as separate Workbooks and Graphs. Finally, the data obtained at different test potentials are combined (**Layer 3**) and analyzed (**Layer 4**) to compute the overall voltage dependence of the time constant of recovery from inactivation, as shown in the “Summary” graph.

This type of analysis is particularly demanding and time-consuming if performed manually (>15 min).

# 6. Investigation of concentration dependence of $I_{Na}$ inhibition by tetrodotoxin using voltage-step protocol



Click  and select file:

**INa\_TTX.dat**

Click 

Dialog box: Select pClamp file  
When prompted one can optionally  
include TTX wash-out data.  
Select file:

**INa\_Wash.dat**

to do this

**Layer 1** shows voltage protocol (here voltage steps from -100 to 10 mV applied at 10 s interval).

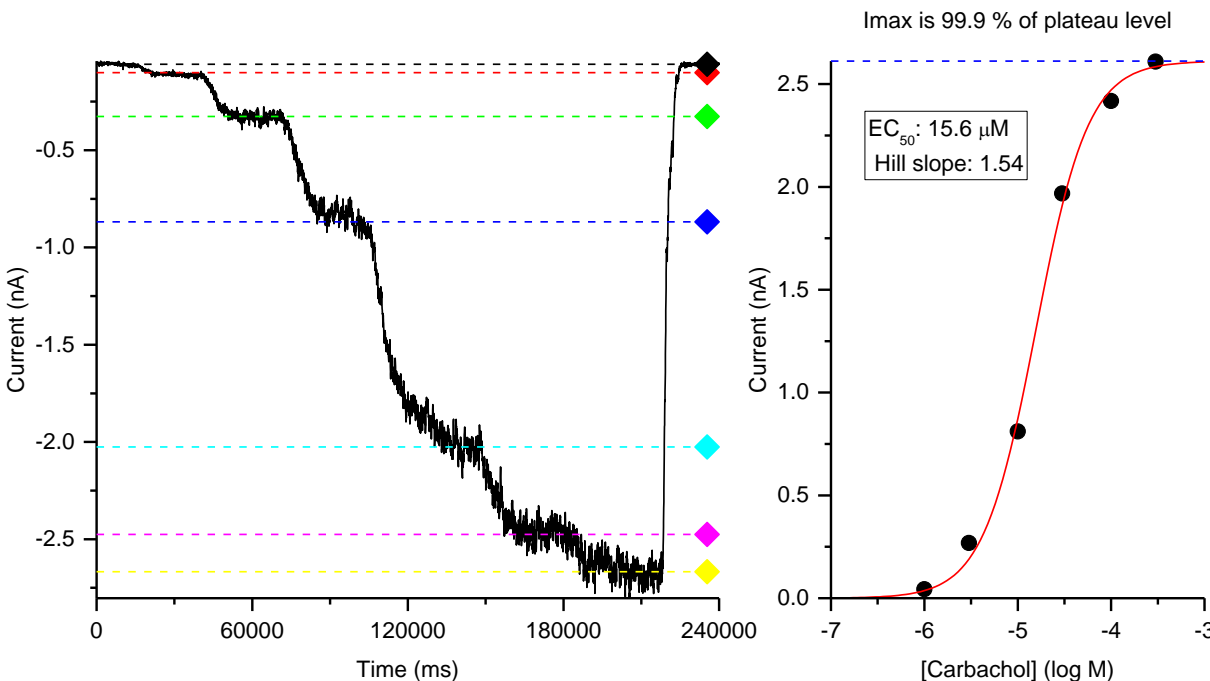
**Layers 2 & 6** show superimposed  $I_{Na}$  current traces recorded during cumulative application of ascending tetrodotoxin (TTX) concentrations as shown in **Layer 3** and after wash-out of the blocker (**Layer 6**).

**Layer 4** shows time course of  $I_{Na}$  inhibition by TTX, followed by wash-out of the sodium channel blocker.

**Layer 5** displays mean (average of the last 5 peak amplitudes at each TTX concentration) normalized by averaged (also 5 values) control current amplitude. Data points are then fitted by the "DoseResp" function (found in "Pharmacology" category of Origin built-in functions) to compute the  $IC_{50}$  value and Hill slope, which are shown in the label.



# 7. Agonist concentration-response curve of the muscarinic cation current ( $ml_{CAT}$ ) – manual mode



Click  and select file:

**CCh\_DR.abf**

Dialog box: Enter number  
Enter 5000

Click 

Click NoDialog box: Auto/Manual

Dialog box: Agonist concentrations  
used (in mkM)

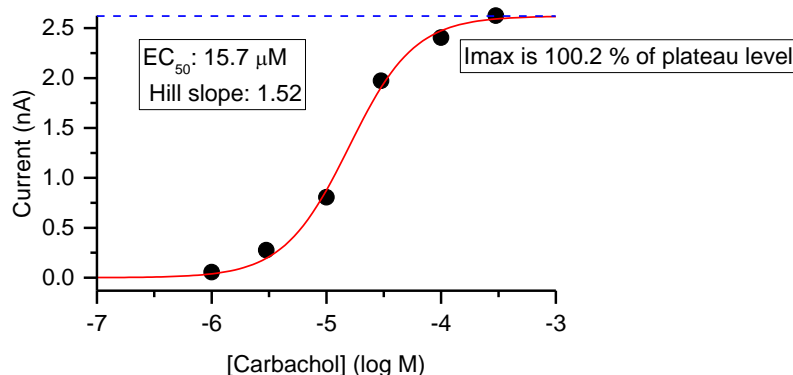
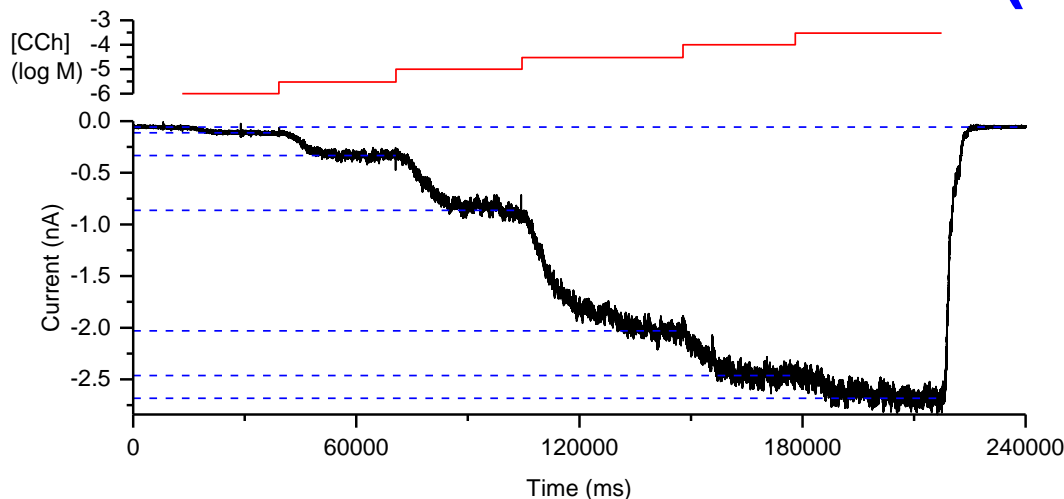
Click Ok to accept the default values  
Position the horizontal cursors as  
shown in Layer 1 and click on the  
“Done” button to continue the script

**Layer 1** shows muscarinic cation current ( $ml_{CAT}$ ) recorded in an ileal myocyte in response to carbachol applied in cumulative manner at 1, 3, 10, 30, 100 and 300  $\mu M$ .

**Layer 2** shows data points fitted by the “DoseResp” function (found in “Pharmacology” category of Origin built-in functions) with the best-fit parameters indicated. In addition, the blue dotted line indicates the best-fit maximal amplitude level. The actual  $I_{max}$  amplitude is also given in % of the latter.

Note that it is very important to get data points at saturating agonist concentrations as fitting partial data by the Hill equation does not produce reliable  $EC_{50}$  and Hill slope estimates. Also note that placing cursors in any particular order is not required since the measured values will be later sorted in ascending order by the script.

# 8. Agonist concentration-response curve of the muscarinic cation current ( $ml_{CAT}$ ) – auto mode



Click  and select file:

**CCh\_DR.abf**

Dialog box: Enter number  
Click Ok to accept the maximal number of data points in this trace

Click 

Dialog box: Auto/Manual  
Click Yes

Dialog box: Enter search parameters  
Click Ok to accept the default values for the width (20) and height (20, in SD values) while searching for peaks

This analysis is generally similar to the above described case 7. However, to automate the various measurements, it takes advantage of the presence of brief current artefacts produced by operation of the solution-changing valves. Thus, prior to the script execution the moments of solution change are seen as rapid vertical deflections on the trace.

Afterwards **Layer 1** shows the application of various concentrations of carbachol, which are plotted on the logarithmic scale. Corresponding time points can be easily located by the peak search routine. Upon its completion the artefacts are masked and the trace is rescaled (**Layer 2**). Next, mean current during 10 s just before each solution application (i.e. after current reaches its state-state level) is calculated (blue horizontal dotted lines are drawn for visual check), baseline current amplitude is subtracted and the resulting current values are plotted against agonist concentration (**Layer 3**). Finally, data points are fitted by the “DoseResp” function, and the best-fit parameters appear in the label.

## For more details of the case studies please refer to the following publications:

### Case 1

Melanaphy D, Johnson CD, Kustov MV, Watson CA, Borysova L, Burdyga TV, Zholos AV (2016). Ion channel mechanisms of rat tail artery contraction-relaxation by menthol involving, respectively, TRPM8 activation and L-type  $\text{Ca}^{2+}$  channel inhibition. *American Journal of Physiology* 311, H1416-H1430.

### Case 2

Fernandez JA, Skryma R, Bidaux G, Magleby KL, Scholfield CN, McGeown JG, Prevarskaya N, Zholos AV (2011). Voltage- and cold-dependent gating of single TRPM8 ion channels. *Journal of General Physiology* 137, 173-195.

### Case 3

Baidan LV, Zholos AV, Shuba MF, Wood JD (1992). Patch-clamp recording in myenteric neurons of guinea pig small intestine. *American Journal of Physiology* 262, G1074-G1078.

Zholos AV, Baidan LV, Starodub AM, Wood JD (1999). Potassium channels of myenteric neurons in guinea-pig small intestine. *Neuroscience* 89, 603-618.

### Cases 4-6

Zholos AV, Fenech CJ, Prestwich SA, Bolton TB (2000). Membrane currents in cultured human intestinal smooth muscle cells. *Journal of Physiology* 528, 521-537.

Zholos AV, Baidan LV, Wood JD (2002). Sodium conductance in cultured myenteric AH-type neurons from guinea-pig small intestine. *Autonomic Neuroscience - Basic & Clinical* 96, 93-102.

### Cases 7-8

Zholos AV & Bolton TB (1997). Muscarinic receptor subtypes controlling the cationic current in guinea-pig ileal smooth muscle. *British Journal of Pharmacology* 122, 885-893.

Yan HD, Okamoto H, Unno T, Tsytsyura YD, Prestwich SA, Komori S, Zholos AV, & Bolton TB (2003). Effects of G-protein-specific antibodies and  $\text{G}\beta\gamma$  subunits on the muscarinic receptor-operated cation current in guinea-pig ileal smooth muscle cells. *British Journal of Pharmacology* 139, 605-615.